

**Performance of reverse osmosis membrane with large feed pressure fluctuations from
simulated wave driven desalination system**

Kurban A. Sitterley¹, Scott Dale Jenne, Yu Yi-Hsiang, Tzahi Y. Cath¹

¹*Colorado School of Mines, Golden, CO*

Abstract:

Wave powered desalination systems (WPDS) are proposed water treatment systems that involve reverse osmosis (RO) of seawater powered directly by wave motion. Such a configuration would result in drastic feed pressure fluctuations. For a technology conventionally operated with a constant feed condition, the effect of these variable pressures on membrane integrity and performance is unknown. This research presents several experiments conducted with a commercially available spiral bound membrane coupled to an experimental system capable of producing feed pressure fluctuations of up to 400 psi. Feed composition included 5, 20, and 35 g/L NaCl, and a synthetic seawater blend (Instant Ocean) at normal and 1.5× concentration. The variable feed conditions included sine-like waves of pressure swings from 200-500 and 500-900 psi with frequencies of 1.25, 7.5, and 12 waves/min as well as a model-generated random waveform. Between each wave experiment, membrane integrity tests were performed at 650 psi and 25 g/L NaCl and showed a drop in the membrane's water permeability coefficient of 7.4%, flux decline of 18.4%, and salt rejection >99% over 1,770 hours of cumulative wave time. Elemental analysis of homogenized permeate samples showed normal rejection efficiencies and acceptable concentrations. In general, variable feed pressure had no significant deleterious effect on membrane integrity or performance. This research takes the first step towards understanding membrane fundamentals under varying feed conditions.

Keywords: desalination, reverse osmosis, hydrokinetic energy, wave energy, sustainability

1. Introduction

The production of drinking water relies on a consistent energy source to perform the necessary treatment. Many places lack one or both of these resources, driving technological innovation to further enable access to safe drinking water. In coastal areas, desalination can play a role in expanding access. Desalination uses a semi-permeable membrane and high hydraulic pressure to remove salt and other contaminants from seawater and brackish water. Often, desalination is too energy intensive to implement in developing coastal communities where reliable energy is scarce for a technology that can require up to 10 times more energy to treat per m^3 than surface water [1]. Thus, there has been much effort into implementing desalination using sustainable and renewable energy sources and doing so can reduce associated airborne emissions by 85% and lower costs for the end user [1, 2]. There have been demonstrations and modelling of systems that use renewable (but intermittent) sources of energy including wind [3-5], solar [6], and geothermal [2].

An often-overlooked source of renewable energy in coastal communities is energy harvested from the motion of ocean waves, or “hydrokinetic” energy. Waves contain an estimated 8,000-80,000 TWh/year of energy – a huge resource, [1] and many devices exist that are capable of converting wave motion to usable energy, termed wave energy converters (WECs). Large population centers located on coastlines, including 14 of the 17 largest cities in the world, have significant potential hydrokinetic energy resources; use of hydrokinetic energy for seawater desalination is a natural progression in the push towards sustainable development of water resources [7]. Typically, wave energy is converted to electricity that is then used to power the desalination system operating at a constant feed pressure [8]. Several reverse osmosis (RO) systems have been designed and built that use hydrokinetic energy in different forms [9-11]. Such systems, broadly called wave driven desalination systems (WPDS), commonly include a wave

activated body (e.g. a buoy or flapping device) driving a fluid (air or water) through a turbine to produce electricity that then powers a feed pump for an RO system.

As the growing population increases demand on the limited global freshwater supply, seawater desalination is an increasingly prominent approach for producing safe drinking water. Research into new desalination membrane technology has been increasing in recent years, resulting in more robust and less expensive membranes that can be tailored to specific applications [12, 13]. Membranes are made with a variety of organic and inorganic materials and are often first characterized by their pore size, with RO membranes having the smallest pores that enable desalination of seawater. These membranes are produced commercially and are typically packaged in a spiral wound module consisting of a flat sheet membrane wrapped around a central tube for collection of permeate.

Though modern membranes are robust, their performance and longevity are highly dependent on the composition of the feed water and the operating conditions of the system. Poor feed water quality, or lack of pretreatment, can induce chemical and biological fouling, reduce the life of the membrane, and result in poor quality permeate [14]. Permeate water quality is also affected by feed pressure because more salt will pass through the membrane as feed pressure approaches the osmotic pressure of the feed water (about 360-435 psi / 25-30 bar for seawater). RO membranes deployed for desalination are conventionally operated with a constant feed pressure to facilitate consistent operating conditions and permeate quality [12]. However, operating an RO system using only wave motion to drive feed pressure would result in a variable feed pressure that changes with the motion of the waves [15]. The power (P) stored in a wave is directly related to the height (H) and period (T) of a wave [9]:

$$P = \frac{\rho g^2 H^2 T}{64\pi}$$

where g is acceleration due to gravity, and ρ is the density of water. As waves become longer and higher, the power available to pressurize water increases. Depending on the location and time of year, wave energy ranges between <10 kW to >120 kW per meter of wave height [16]. Clearly, in the ocean's dynamic wave system, feed pressure using only a WEC would not be constant. Because most membranes are designed with constant feed pressure in mind, and because there is no apparent reason or advantage to running with variable feed pressure, the effect of such variable pressures on membrane integrity and performance is unknown. Feed pressure contributes to the net driving pressure (NDP) in a membrane system, which is the sum of all the forces acting on the membrane. Feed pressure is typically the largest value used when calculating NDP and impacts not only the physical integrity of the membrane, but many other performance characteristics of RO systems including permeate flow rate, permeate quality, and recovery. Membrane fouling mechanisms are different at low and high pressures as well; low pressures typically produce internal fouling such as pore clogging, while high pressures produce external fouling like scaling [14]. The extent that each of these occur in a system operating at variable feed pressure is unknown and must be understood to run a successful system.

Literature on variable feed pressure with RO is limited to studies conducted on “pulsed” RO to mitigate concentration polarization effects and improve performance [17-22]. Kennedy et al. [22] tested a variety of conditions and saw a maximum increase of 70% in permeation flow. Abbas and Al-Bastaki modified, validated, and improved the model proposed in Kennedy et al. and demonstrated improved permeate flow and salt rejection afforded by pulsed RO in the form of square and asymmetrical waveform pressure pulses [17, 20, 21, 23]; these results were attributed to the reduction in the effect of concentration polarization [24]. However, in these studies, the focus was on model validation and process optimization without regard for the impact to

membrane integrity over longer periods of operation. Short experiments (30 minutes) using square waves were conducted using either sucrose or 10 g/L NaCl. These studies provide no guidance for potential impacts to membrane integrity that could result from wave driven variable feed pressure for desalination of seawater.

There has been some WPDS modelling [8, 15, 25] of systems that include devices like WECs, pressure relief valves, and other energy saving and recovering mechanisms. While these models do consider some of the logistics and economics of implementing such a system, there is no mention of the impact of the variable feed pressure conditions on membrane integrity and long-term performance. There has also been no known pilot-scale assessment of these conditions on RO membranes and understanding them is essential to implementing a WPDS. Typical tests for comparing high performance RO membranes are done with a 32,000 mg/L NaCl feed solution at 800 psi (55.1 bar) and 25 °C [26]. In a purely wave-driven system, however, modelled systems' feed pressure can range between 290-1740 psi (20-120 bar) [25]. It is impossible to take performance data from a constant feed pressure test and extrapolate it to apply to such a scenario. Because our water treatment and delivery systems are inherently life-sustaining, it is paramount that their long-term behavior and performance is predictable to a certain degree. For an RO system operating in open ocean under variable conditions, understanding the impact on the membrane is germane to performance predictability, particularly if this system is to operate in a developing community with limited resources. Before further development or implementation of a purely wave-driven RO system, there must be fundamental research considering if the membrane can handle the abuse of irregular feed conditions and any impact on permeate quality. To investigate the impact of variations in feed pressure on membrane integrity and permeate quality, this research

presents results from several experiments with different feed compositions and wave conditions on a commercial RO membrane and elemental analysis of the product water.

DRAFT

2. Materials & methods

2.1 System construction/flow

A flowchart of the system used to conduct these experiments is pictured in Figure 1 and was fabricated at the Colorado School of Mines. Feed water from the feed tank flows by gravity to a pump (Hydra-Cell M03; Minneapolis, MN). The feed water is pumped through an in-line pressure sensor and heat exchanger to the pressure vessel containing a Dow Filmtec SW30-2540 RO membrane with an active area of 2.8 m². The reject stream flows back to the feed tank through a back-pressure valve, flow meter, and conductivity cell. The permeate stream also flows through a flow meter and conductivity cell back to the feed tank. Feed water temperature is regulated by flowing through a heat exchanger connected to a chiller. Each of the sensors (pressure, conductivity, flow) are connected to a system control and data acquisition system (LabJack; Englewood, CO) to provide visual interface with the experimental setup. The feed pressure sensor was calibrated using an in-line analog pressure gage and conductivity probes were calibrated with traceable conductivity standards (Fisher Scientific International Inc.; Pittsburgh, PA).

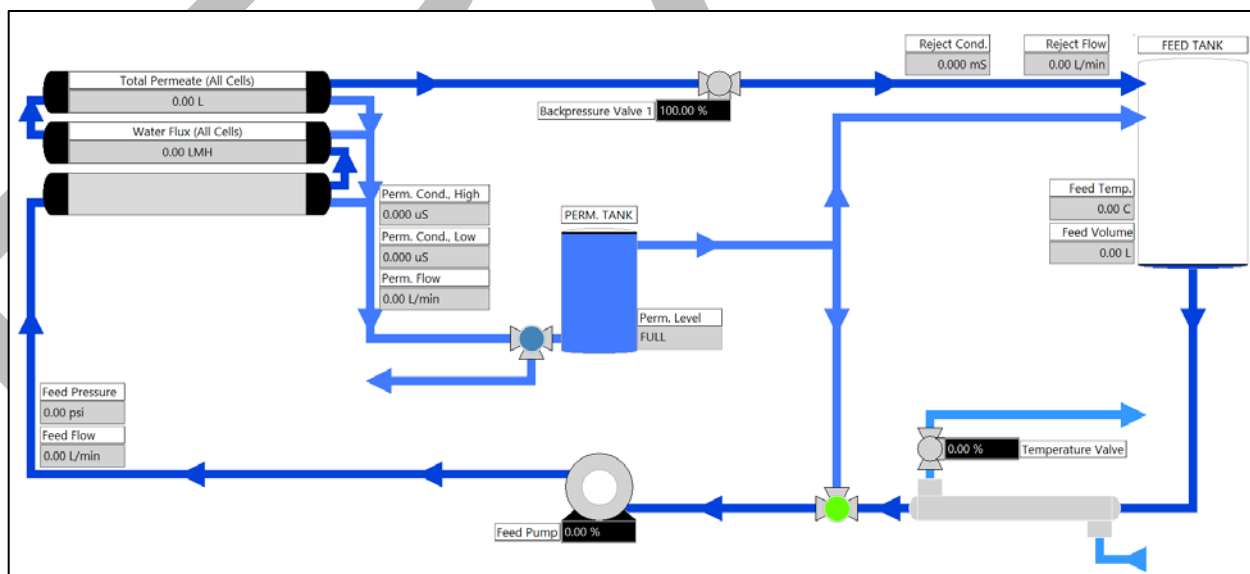


Figure 1: Flow diagram for experimental system. Note that the system was equipped with a separate tank to collect permeate, but it was not used for these experiments and permeate was redirected to the feed tank.

2.2 Experimental design

Experiments were of two kinds: wave and integrity. Wave experiments simulated wave motion, and these were further broken down into three regimes: (1) constant flux ($J_w = 15$ LMH) for 1 hour at the beginning of each experiment, (2) wave form for 7 days, (3) repeat constant flux for 1 hour at the end. Several experiments were conducted with this basic format with different feed compositions and wave periods. The feed composition for wave experiments included 5-35 g/L NaCl and Instant Ocean (Spectrum Brands Holdings Inc.; Madison, WI), a commercially available synthetic seawater blend. Integrity tests used 25 g/L NaCl feed held at 650 psi (44.8 bar) for 2 hours and were performed in between wave experiments as a control to monitor any degradation in membrane performance. Table 1 contains a summary of all experiments performed. Throughout the experiments with Instant Ocean, permeate samples were collected for elemental analysis.

Sine-like wave motion was simulated by setting the feed pressure range, wave period, and wave frequency for the system to simulate. Guidance for the range of feed pressures was taken from Yu and Jenne [15, 25], which included simulations of a WPDS. Three waves were chosen: 1.25 waves/min (48 s wave period, slow), 7.5 waves/min (8 s wave period, medium), and 12 waves/min (5 s wave period, fast). These wave periods span the spectrum of what might reasonably be experienced near a coastline where a WPDS might operate and to simulate the operating conditions for a system that includes devices such as WECs, pressure accumulators, and pressure relief valves that have the effect of “smoothing” the feed pressure form, as have been present in some simulations [8, 15, 25, 27]. In total, we performed 15 experiments under controlled, sine wave-like conditions. Nine of those were conducted for 7 days, and six were conducted for 24

hours. The latter were performed at a higher frequency of data collection to have higher data resolution on the differences in performance under the three different conditions. Finally, one experiment was performed using feed pressure output from a simulation of a WPDS using real wave height data in Yu and Jenne [15, 25]. Researchers developed a numerical model from WEC-Sim, a Matlab powered time-domain, radiation-and-diffraction-based numerical tool to evaluate the performance and cost of a WPDS in the United States. The modeled system had several forms and included a WEC, a hydraulic accumulator, and a pressure exchanger. Numerically modelled interactions between these components provided output of the feed pressure to an RO system based on real wave height data from a buoy in northern California. The feed pressure in the model was set to be constrained by the upper limit on operational feed pressure for the modeled membranes, resulting in a wave form with pressure fluctuations between 575-800 psi (39.6-55.2 bar).

2.3 Membrane integrity

The water permeability coefficient (A , $\text{m s}^{-1} \text{bar}^{-1}$) was the metric used to evaluate if the membrane integrity had diminished as a result of the wave experiments. This parameter was calculated for each data point according to:

$$A = \frac{J_w}{P_F - \left(\frac{\pi_F + \pi_R}{2}\right)}$$

where J_w is water flux (m s^{-1}), P_F is feed pressure (bar), π_F is osmotic pressure of feed solution (bar), and π_R is osmotic pressure of the reject (bar). For this calculation, both pressure drop across the membrane (i.e.) and permeate hydrostatic and osmotic pressure was assumed to be negligible (i.e. $P_{F,out} = P_{F,in}$ and $P_{perm} = \pi_{perm} = 0$). Osmotic pressure of the feed was estimated with the Lenntech web-based calculator and then π_R was calculated assuming it scaled linearly with conductivity throughout the experiments:

$$\frac{\pi_F}{C_F} = \frac{\pi_R}{C_R}$$

2.4 Analytical procedures

Samples were collected from the permeate stream and analyzed for cations using inductively coupled plasma optical emission spectrometry (PerkinElmer Avio 200 ICP-OES) with an in-house method developed to be similar to Standard Method 3120 and for anions using ion chromatography (Dionex ICS-90) with Standard Method 4110B. Instant Ocean was used as a synthetic seawater and includes B, Ca, K, Mg, Na, and Sr in their blend at concentrations intended to be close to seawater. Samples were collected from the permeate stream during the start and end constant flux periods, and throughout the wave phase. The samples collected during the wave phase were collected over the duration of one full wave and homogenized before being placed in a sample container and analyzed for major cations (B, K, Na, Ca, Mg, Sr) and select anions (Cl, Br). The average feed solution composition for these analytes is presented in the supporting information as Table SI-1.

2.5 Data processing procedures

Data files were outputted from the experimental setup as a .csv file, imported into Matlab (version R2019a, The MathWorks Inc.; Natick, MA), and processed using an application developed in-house. The application took estimations for osmotic pressure and feed conductivity to produce estimations for other values, such as the salt and water permeability coefficients. Simple functions to calculate mean and standard deviation were used to determine these values over run time durations that corresponded to either a constant flux period or a wave period. Initial startup and ramp up portions of each experiment were not included in these calculations. In some cases,

instrument noise caused calculated value data points (i.e. data points that were not measured but rather calculated *a posteriori* such as the water permeability coefficient) to have significant deviation from expected values based on data points immediately before and after. When this was the case, the Matlab find function was used with logic to exclude these from calculations of descriptive statistics.

3. Results & Discussion

3.1 Membrane performance and integrity under wave conditions

3.1.1 Sine waves

The average and standard deviation for pressure, flux, temperature, permeate conductivity, salt rejection, water permeability coefficient, salt permeability coefficient (B), and percent recovery are summarized in Table 1 for the 7 day experiments. These values represent the average of data points collected every 1 min for the duration of the experiment. The system was set to maintain a temperature of 19-20 °C, and the average across all experiments in Table 1 was 19.7 ± 0.6 °C. Pressure for each experiment is the average of the high- and low-pressure settings of the sine wave; for these experiments, the waves were sinusoidal and the system spent equal times ramping up and down to the peak and trough of the simulated wave motion. Flux, permeate conductivity, water permeability coefficient, salt permeability coefficient, and recovery averages for each experiment changed as expected with changes in feed salinity and pressure settings (e.g., lower average flux resulted in E3 due to higher feed salinity run at same conditions as E2) and signal no obvious indication of membrane damage due to the waves (differences due to variations in wave frequency are discussed later). Not surprisingly, the standard deviation on these performance parameters are larger than those for integrity tests owing to the variation in the feed pressure.

Table 1. Condition, pressure, flux, temperature, permeate flow, permeate conductivity, salt rejection, water permeability coefficient (*A*), salt permeability coefficient (*B*), and percent recovery for sine wave experiments conducted for 7 days.

Conditions	Designation	Pressure (psi)	Flux (LMH)	Temp. (°C)	Perm. Flow (L min ⁻¹)	Perm. Cond. (μS cm ⁻¹)	Salt Rej. (%)	A (m s ⁻¹ bar ⁻¹)	B (m s ⁻¹)	Recovery (%)
5 g/L NaCl 200-500 psi 7.5 wave/min	E2	350±120	25.6±10.0	19.3±0.3	1.1±0.4	30±3	99.7±0.0	3.7±0.3×10 ⁻⁷	1.4±0.7×10 ⁻⁸	21.0±5.8
20 g/L NaCl 200-500 psi 7.5 wave/min	E3	360±110	10.1±7.5	19.1±0.4	0.5±0.3	400±60	98.9±0.2	3.8±0.2×10 ⁻⁷	2.3±1.9×10 ⁻⁸	8.5±5.5
35 g/L NaCl 500-900 psi 7.5 wave/min	E4	720±150	18.4±9.3	19.5±0.3	0.8±0.4	865±75	98.6±0.1	2.6±0.6×10 ⁻⁷	5.9±3.0×10 ⁻⁸	12.9±5.1
35 g/L NaCl 500-900 psi 1.25 wave/min	E5	710±150	18.5±8.4	20.3±0.4	0.8±0.4	550±60	99.1±0.1	2.6±0.5×10 ⁻⁷	3.5±1.8×10 ⁻⁸	12.5±4.8
35 g/L NaCl 500-900 psi 12 wave/min	E6	710±140	18.4±10.1	19.2±0.1	0.8±0.5	785±105	98.7±0.2	2.7±0.8×10 ⁻⁷	3.7±2.7×10 ⁻⁸	11.4±5.1
Instant Ocean 500-900 psi 7.5 wave/min	E7	680±170	24.3±11.3	20.2±0.4	1.1±0.5	415±45	99.1±0.1	3.8±0.9×10 ⁻⁷	4.4±2.1×10 ⁻⁸	16.0±5.4
Instant Ocean 500-900 psi 1.25 wave/min	E8	700±140	24.5±8.6	20.2±0.3	1.1±0.4	250±30	99.5±0.1	3.7±0.9×10 ⁻⁷	2.7±1.1×10 ⁻⁸	16.6±3.8
Instant Ocean 500-900 psi 12 wave/min	E9	700±150	23.4±10.6	20.4±0.2	1.1±0.5	300±15	99.4±0.0	3.7±0.8×10 ⁻⁷	3.0±1.3×10 ⁻⁸	15.8±5.2
1.5× Instant Ocean 500-900 psi 7.5 wave/min	E12	700±150	13.2±8.9	20.3±0.5	0.6±0.4	740±95	98.9±0.1	4.2±2.4×10 ⁻⁷	3.1±2.1×10 ⁻⁸	8.2±4.8

Comparing all nine of these experiments to each other is not sensible owing to their different feed conditions, but for those experiments with identical feed salinity and wave form pressure ranges (e.g. E4-E6 and E7-E9), we can examine the impact that wave frequency had on performance. There is a relationship between the period of the wave and permeate conductivity. The experiments with the longest period (1.25 wave/min, E5 and E8) resulted in permeate with the lowest average conductivity (550±60 μS/cm and 250±30 μS/cm, respectively) and those with shorter periods gave higher average permeate conductivity. For both feed compositions (Instant Ocean and 35 g/L NaCl), the mid wave frequency of 7.5 wave/min (E4 and E7) caused the highest average permeate conductivity (865±75 μS/cm and 415±45 μS/cm, respectively) within each group and the permeate for those experiments with the shortest period of 12 wave/min (E6 and E9) fell in between (785±105 μS/cm and 298.8±15.0 μS/cm, respectively). This concept is more fully discussed in a later section.

It is difficult to compare the results of these experiments to the typical operating parameters of full-scale desalination plants because there are no full-scale plants that use variable feed pressures at this magnitude. Nevertheless, it is worth comparing these results to what is typical for seawater desalination plants. The results presented in Table 1 for the wave experiments compare favorably to performance of full-scale desalination plants. Conventional seawater desalination plants that use a single stage and single pass configuration operate with a flux of 12-17 LMH between 5500-8000 kPa (800-1100 psi / 55.2-75.8 bar) and achieve recoveries around 35-45% with permeate TDS <500 mg/L [28, 29]. Desalination systems using hydrokinetic energy have reported recoveries of 33-37% [10]. Recoveries were lower in these experiments but would be increased by increasing the range of operating pressure and including additional membrane elements, but this would increase the specific energy consumption for the system and might not be achievable with a purely wave-driven desalination system [29]. Wave-driven feed pressures as high as 1800 psi (125 bar) were achieved in simulations done by Yu and Jenne [25] of a system without hydraulic accumulators or pressure relief valves, but were confined to 725-870 psi (50.0-60.0 bar) when these components were included. In separate analysis, their desalination model targeted 70 ppm permeate quality with a higher targeted feed pressure of 1000 psi (68.9 bar) [15]. However, targeting higher recoveries seen in conventional RO plants may not achieve the best results. Folley et al. [8] simulated a wave-powered RO plant that used a pressure exchanger-intensifier to facilitate a maximum recovery of 25%. Analysis of the results showed that higher recovery by using more membranes resulted in lower quality permeate and diminishing returns for recovery while increasing the specific energy consumption. While these results reflect a specialized configuration of a simulated system, with better understanding of the variable feed pressure on membrane integrity a deployed system could be optimized to produce conditions that protect the integrity and

longevity of the membrane while also producing high quality permeate. Additionally, achieving higher pressures and efficiencies in a purely wave driven system would be highly dependent on local wave conditions.

Water permeability coefficient, salt permeability coefficient, and permeate conductivity are shown in Figure 2 for the beginning and ending constant flux periods of the 7 day experiments. The approach taken for these experiments was to gradually change experimental conditions, initially keeping salinity low (5 g/L NaCl) and the same wave frequency (7.5 wave/min) before gradually increasing the salinity and wave pressure and varying the wave frequency. Figure 2 shows that there was no significant change in water permeability as a result wave motion for each of the nine experiments. There is a decrease in water permeability with increasing feed concentration due to the increased pressure needed to maintain constant flux. Likewise, the salt permeability and permeate conductivity did not change considerably between the beginning and end of each 7 d experiment. Both tracked with expected changes due to changes in feed composition (e.g. increasing for higher feed salinity). An exception to this is the results from the 7.5 wave/min experiment conducted with 35 g/L NaCl. Permeate conductivity (and therefore, salt permeability coefficient) was observed to increase over the course of the experiment and was reflected in the results in Figure 2. This result is not consistent with the other results that show no significant change in these parameters from the beginning to the end of the experiment. There is no noticeable trend in these parameters with respect to change in wave speed from experiment to experiment; the only observed changes occur with a change in feed composition.

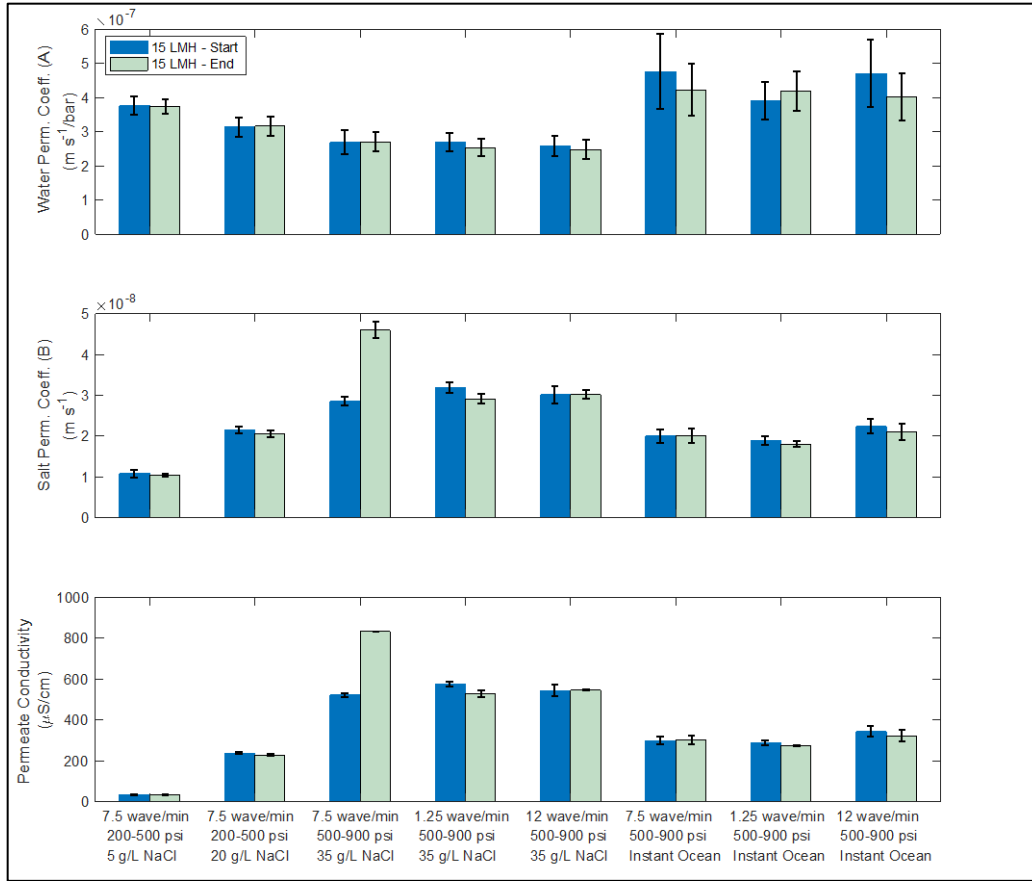


Figure 2. Water permeability coefficient (A, top frame), salt permeability coefficient (B, middle frame), and permeate conductivity (bottom frame) for the beginning and end constant flux period for each sine wave, 7 day experiment.

The pressure (top frames, red), flux (middle frames, blue), and permeate conductivity (bottom frames, green) are shown in Figure 3 for 0.1 hour of operation for the three wave conditions. The purple line on the pressure and flux plots represent the average pressure and flux, respectively for these experiments. The plots show the variation in permeate quality and flux that can result from different wave conditions. Waves at 1.25 wave/min produced flux between 10.1-38.1 LMH and permeate conductivity between 330-405 $\mu\text{S}/\text{cm}$, 7.5 wave/min between 7.5-43.3 LMH and 425-440 $\mu\text{S}/\text{cm}$, and 12 wave/min between 6.8-39.7 LMH and 515-530 $\mu\text{S}/\text{cm}$. In each plot, the observed double hump is the point at which the system restarted the wave cycle. When the cycle restarted, the system sustained a higher pressure for longer, resulting in permeate conductivity dips

observed for all three wave conditions. The slowest waves produced the lowest conductivity permeate but also the widest fluctuations in permeate quality while faster waves produced lower quality permeate with smaller fluctuations. As seen in Figure 3, the slowest waves more consistently hit the intended pressure range of 500-900 psi (34.5-62.1 bar) than the medium and fast waves, resulting in a slightly higher average pressure (726 psi / 50.1 bar) for these experiments that could partially explain the differences in permeate conductivity.

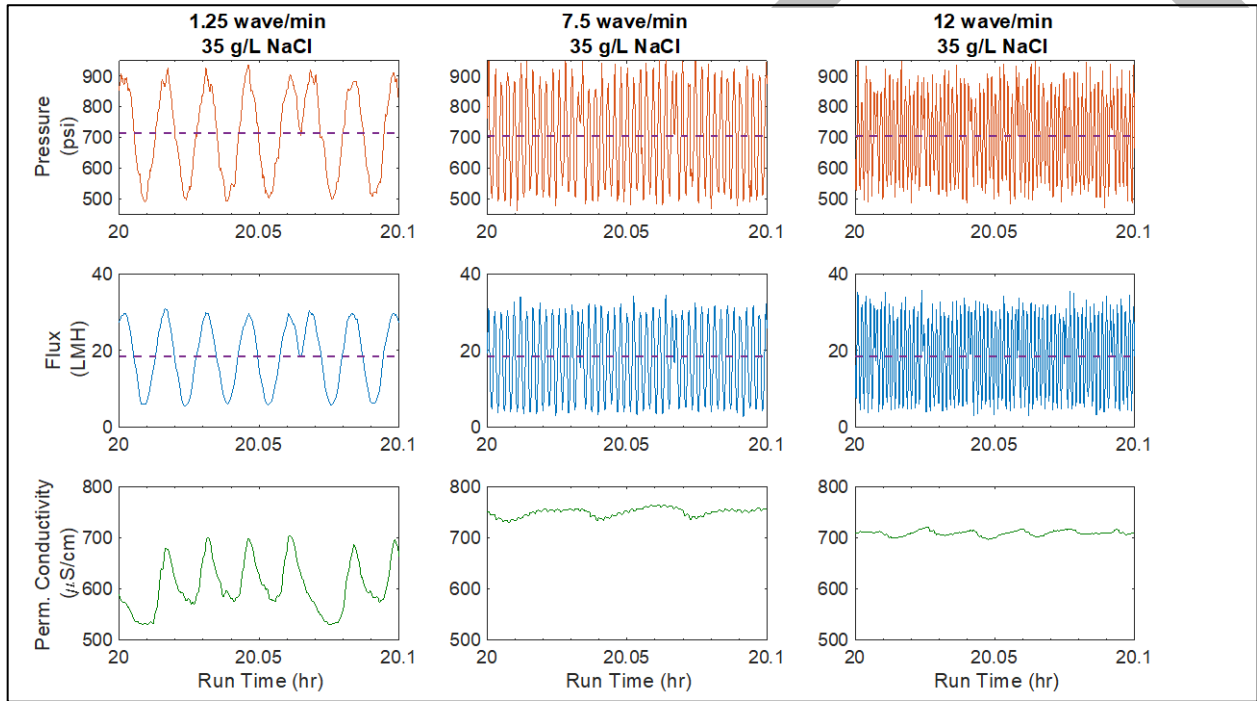


Figure 3. Pressure, flux, and permeate conductivity for 0.1 hr of run time for experiments with 1.25 wave/min (left frames), 7.5 wave/min (middle frames), and 12 wave/min (right frames).

These results show the impact that the sea condition could have on permeate water quality and highlight how low-pressure swings can cause major swings in permeate quality. Lower permeate conductivity in the slowest wave form can be interpreted through the relationship between power generated per unit wave crest, wave height, and wave period, as described in the introduction [30].

The wave period, T , is related to the wavelength λ by:

$$\lambda = \frac{gT^2}{2\pi}$$

and H is related to the wavelength by the wave slope factor, β :

$$\beta = \frac{\lambda}{H}$$

Substitution and rearrangement lead to:

$$P = \frac{\rho H^{2.5}}{64} \sqrt{\frac{2g^3}{\pi\beta}}$$

Because β typically falls between 0.03-0.05, and taking the other constants into consideration, this relationship can be approximated as $P = 2H^{2.5}$. Thus, sea conditions with waves with longer periods result in more powerful waves that would generate a higher feed pressure for RO system. In simulations of wave-driven RO done by Yu and Jenne [25], wave environments with higher periods and higher significant wave heights yielded higher recoveries and lower permeate concentrations. In their simulations, hydraulic accumulators and pressure relief valves were included to modulate the feed pressure between the designed operation range for the membrane (610-825 psi / 42-57 bar). When the pressure exceeded this range, these components had the effect of holding feed pressure constant at the high end of this range until wave height lowered and the pressure fell. This high wave energy simulation environment is most akin to the slowest waves modeled in this research (1.25 wave/min, E5 and E8 in Table 1) because those simulations held the highest-pressure constant for an extended period of time over other simulations in lower energy wave environments. Similarly, the faster waves (7.5 wave/min and 12 wave/min, E4, E6, E7, and E9 in Table 1) more closely resemble the lower energy wave environments from those simulations. Each of the wave experiments in this research produced water with estimated TDS <350 mg/L, but these results coupled with those in Yu and Jenne [25] highlight the impact that the ocean

conditions can have on this type of an RO system. Further, the results shed light on possible complications when trying to deploy a WPDS due to the dependence on local wave conditions.

3.1.2 Variable feed composition

The first 24 hours of two separate experiments conducted under identical wave conditions (7.5 wave/min, 500-900 psi / 34.5-62.0 bar), but different feed compositions, are shown in Figure 4. This period of time includes the initial 15 LMH constant flux period followed by the wave form. The left two panels show the flux and permeate conductivity for a feed with Instant Ocean with averages over the wave portion (i.e. $t \sim 1.5$ -24 hr) of 25.7 ± 10.4 LMH and 415 ± 45 $\mu\text{S}/\text{cm}$, respectively. The right two panels show the flux and permeate conductivity for a feed of $1.5 \times$ Instant Ocean with averages over the wave portion of 13.5 ± 9.2 LMH and 940 ± 90 $\mu\text{S}/\text{cm}$, respectively, over the wave portion. For both experiments, coming out of the constant flux period causes the permeate conductivity to change with the feed pressure. For the experiment with $1.5 \times$ Instant Ocean, this causes an initial rise in permeate conductivity because the pressure needed to hold 15 LMH at this concentration (740 ± 35 psi / 51 ± 2.5 bar) is higher than the beginning of the wave experiment at 500 psi (34.5 bar); thus, there is a brief period of forward osmosis, causing increased permeate conductivity as the system adjusts to these conditions. During the wave portion of these experiments, membrane performance parameters stayed consistent. While this is a result of this system operation, it also provides insight into the large changes in permeate quality that could occur with large pressure swings that could happen in a deployed system as the feed pressure varies with sea conditions. For each experiment, there was a period after switching from constant flux to wave mode where permeate conductivity would adjust to the wave conditions, but after reaching a steady state point, it would not change dramatically for the remainder of the experiment.

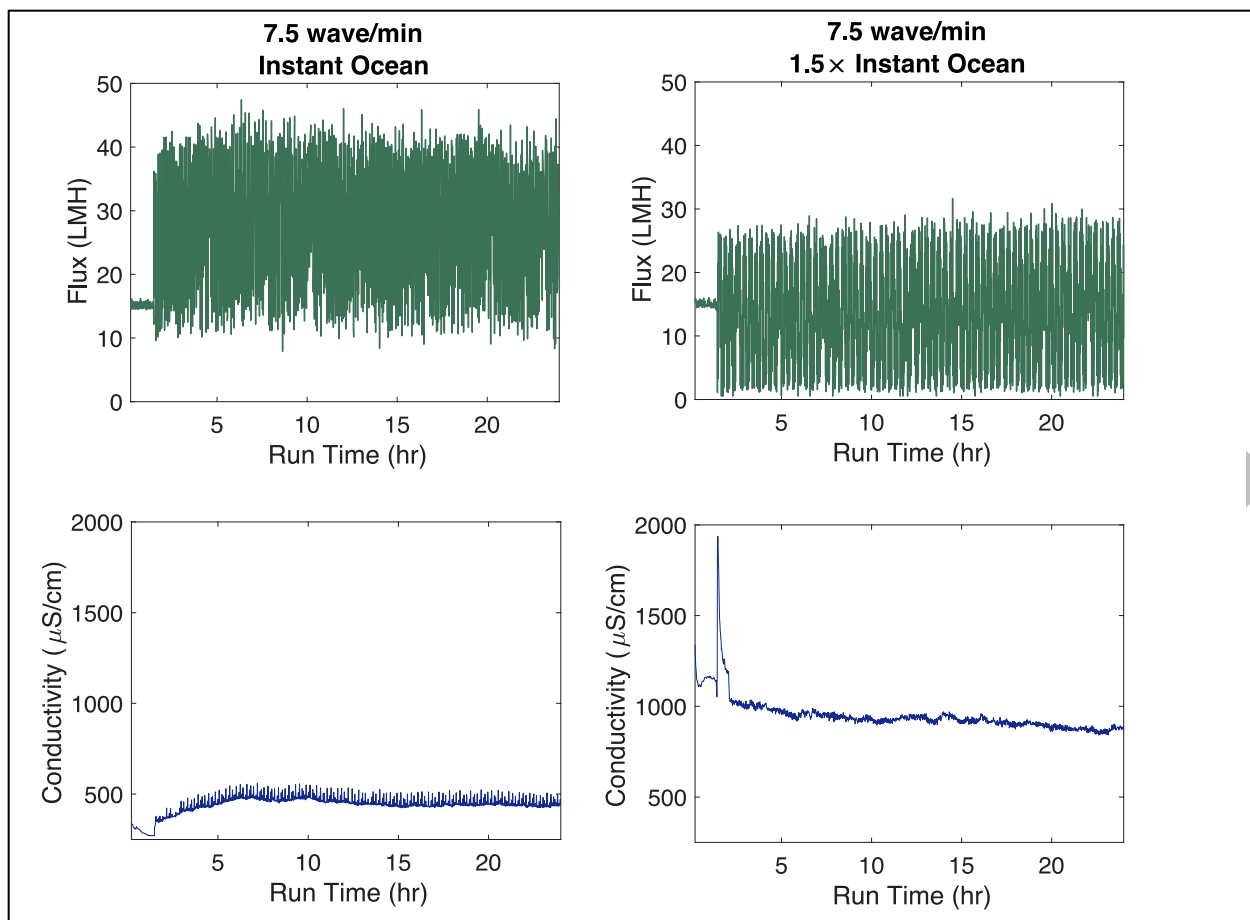


Figure 4. First 24 hr of experiments conducted at 500-900 psi (34.5-62.0 bar) and 7.5 wave/min with Instant Ocean (left frames) and 1.5× Instant Ocean (right frames).

The nature of the wave at these higher feed concentrations has a negative effect on permeate conductivity. The osmotic pressure of the 1.5× Instant Ocean feed is estimated to be 575 psi (39.6 bar). Because this is larger than the lowest pressure of the wave (500 psi / 34.5 bar), there is forward osmosis of water (i.e., water moving from the permeate to feed side of the membrane) during the trough of the wave, causing an increase in permeate conductivity. Conversely, at the highest pressure of the wave (900 psi / 62.1 bar), water flux increases and has the effect of diluting the permeate and bringing the conductivity down. Dipping into forward osmosis periodically with lower feed pressures has been recently explored as a method for membrane backwashing to remove

some scale from the membrane surface [31, 32], but the impact of doing it frequently is unknown. In a deployed system, this should be avoided to improve the quality of the permeate water, as the permeate conductivity is much higher in the experiment with concentrated seawater. In these controlled wave conditions, permeate conductivity is somewhat balanced by the peak and trough of the wave, but the more chaotic conditions of actual wave conditions would cause significant variation in permeate quality, as shown in Figure 3 and in simulations done by Folley et al. [8] and Yu and Jenne [25].

The experimental conditions depicted in Figure 4 is an approximation of conditions in a multi-stage configuration for WPDS. Assuming a multi-stage single-pass configuration and that feed pressures are the same in each stage due to wave motion, as the feed pressure goes below the osmotic pressure of the feed solution, there will be a detriment to permeate quality. Further complicating this multi-stage scenario, the osmotic pressure of the feed would not be constant because like the permeate salinity, reject salinity varies with wave motion. This is in contrast to conventional multi-stage configurations operating under constant pressure where the feed for the second stage would be predictable and constant. In theory it is possible to amplify applied wave pressure in subsequent stages to avoid this effect, but it might require more sophisticated equipment to implement, thus increasing cost, operating difficulty, and system size, detracting from the potential of a WPDS to be deployed in coastal developing communities. Previously mentioned models [8, 25] that simulate a similar system assume single-pass configurations; thus, it is unclear how a multi-pass configuration might affect system design and operational efficiency.

One reason often given for including multiple stages is that it will increase recovery, thus reducing the volume of brine that needs to be disposed and reducing disposal costs [29], which can account for 5-33% of the total cost of the process [33]. Brine streams contain high

concentrations of dissolved solids and pretreatment chemicals, if they are used, and there are negative environmental effects associated with each brine disposal method [33]. Most likely, a WPDS would be situated near to the WEC (e.g. on the seabed) so the most suitable method for brine disposal would be to discharge directly in the surrounding ocean. Much of the cost associated with brine disposal to surface water is transport to the disposal site, typically from a distant location [33]. In this regard, the cost of brine disposal for a WPDS system would be limited to the nominal cost of piping infrastructure needed to get the brine a sufficient distance from the RO intake. The cost of the brine disposal approach should be weighed against the increased cost of adding membrane elements and other system components necessary to increase recovery. Provided that the permeate is of sufficient quality, it is possible that this cost is higher than the additional brine disposal associated with lower recovery and a less complicated system overall.

3.1.3 Random wave conditions

The feed pressure, flux, and permeate conductivity for one cycle of a randomly generated waveform are shown in Figure 5. A plot of the targeted wave form obtained from NREL is shown in the supporting information as Figure SI-1. Further details of the modelled system are available in the publication [25]. The feed pressure output from the model used in this experiment was a total of 50 minutes that was looped over itself continuously for 14 days. Dotted lines on each plot represent the average value for the entire experiment. Average flux was 21.7 ± 3.1 LMH, pressure was 730 ± 60 psi (50.3 ± 4.1 bar), and permeate conductivity was 460 ± 30 $\mu\text{S}/\text{cm}$, similar to the values for the sine-like wave experiments performed (see Table 1). The water permeability constant was $3.1 \pm 0.5 \times 10^{-7}$ $\text{m s}^{-1} \text{bar}^{-1}$, similar to that of the sine-like wave experiments performed, while recovery and salt rejection were $24.1 \pm 2.4\%$ and $99.0 \pm 0.1\%$, respectively.

Despite the slightly lower average water permeability constant, recovery in this experiment was markedly higher than the previous experiments conducted with Instant Ocean. This is likely due to changes in system backpressure valve settings resulting in different feed flow rates in the experimental system that were made to aid the system in more accurately reproducing the higher degree of randomness in this wave form compared to the simple sine wave from previous experiments. Permeate conductivity shows a similar relationship to feed pressure as we saw in the slowest sine-like waves (1.25 wave/min) and was much more variable than seen with slower waves (7.5 and 12 wave/min; see Figure 3). During times of higher pressure (e.g., around $t = 100.1$ hr in Figure 5), we see higher flux and thus higher permeate flow, causing permeate conductivity to decline. When the system experiences the sudden drop in pressure seen around this time, permeate conductivity rises as permeate flow decreases. In this plot, permeate conductivity swings approximately $100 \mu\text{S}/\text{cm}$, which corresponds to a change in TDS of $80 \text{ mg}/\text{L}$. These permeate quality results are consistent with simulations done by Folley et al. [8] and Yu and Jenne [25], thus providing some experimental validation to these model results. Folley et al. present a model with product water with 200-400 ppm salinity with feed pressure of 550-800 psi (38.0-55.0 bar), very similar to the experiments conducted here, though their model was for a system with 165 membranes. Yu and Jenne used a pressure range of 610-810 psi (42.0-57.0 bar) in their model of 183 membranes producing water with 120-380 ppm salinity (depending on sea state). In these models, researchers assigned a maximum pressure at which to engage the pressure relief valve on their modelled system. While many membranes typically are assigned a maximum operating pressure, this is assumed to be for continuous, not intermittent, operation. The commercial membrane used in these experiments (Dow Filmtec SW30-2540) has a maximum operating pressure of 1000 psi (69 bar). However, several experiments were cut short when the system

caused a pressure spike to >1100 psi with no apparent damage to the membrane. It would be useful to better understand the upper limits of pressure membranes can sustain acutely, as this could produce a product water with lower salinity. Higher feed pressure typically results in higher quality permeate, so allowing for times with higher peak pressure during system operation could balance out when the sea state is calmer and producing lower feed pressures and saltier permeate.

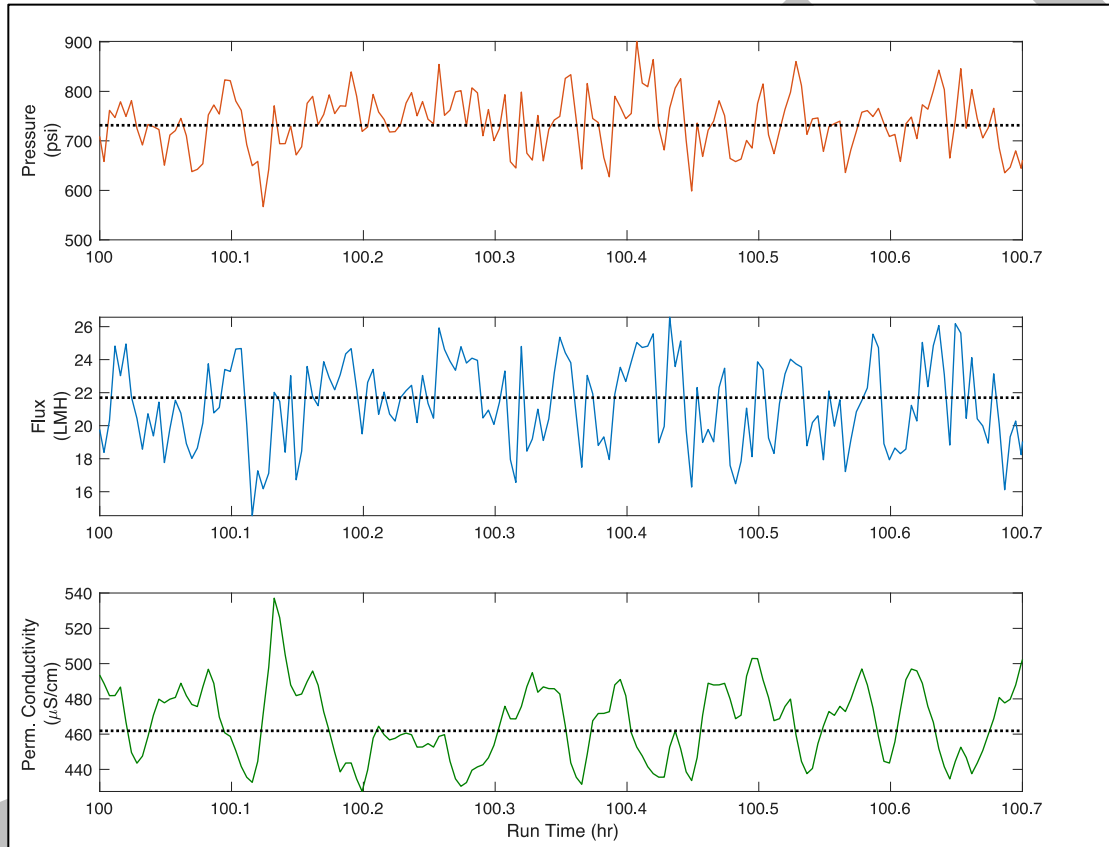


Figure 5. Pressure (red line, top frame), flux (blue line, middle frame), and permeate conductivity (green line, bottom frame) for 1 cycle (approximately 50 minutes) of a randomly generated wave form.

3.2 Membrane integrity

The water permeability coefficient, flux, and salt rejection averaged over the last hour of each integrity test plotted against the total wave time at each point are shown in Figure 6. The total wave time is the total number of hours that the membrane had been subject to wave-like conditions up

until that integrity test. These experiments were conducted in between wave tests to use as a metric to evaluate membrane integrity under identical conditions. Data was collected once every 60 s during these integrity tests, so each point in Figure 6 represents the average and standard deviation of 60 data points. The membrane was subject to a total of 1,770 hrs of wave action and the water permeability coefficient showed no appreciable change after membrane compaction in each integrity test. Water permeability coefficient was initially $3.1 \pm 0.2 \times 10^{-7} \text{ m s}^{-1} \text{ bar}^{-1}$ for compaction and dropped 7.4% to $2.9 \pm 0.3 \times 10^{-7} \text{ m s}^{-1} \text{ bar}^{-1}$ by the last integrity test. There was a more significant drop in flux, with compaction at $28.3 \pm 0.9 \text{ LMH}$ and dropping 18.4% to a low of $23.0 \pm 0.8 \text{ LMH}$. Salt rejection stayed $>99\%$ for all integrity tests with the exception of one, where it dropped to 98.9%.

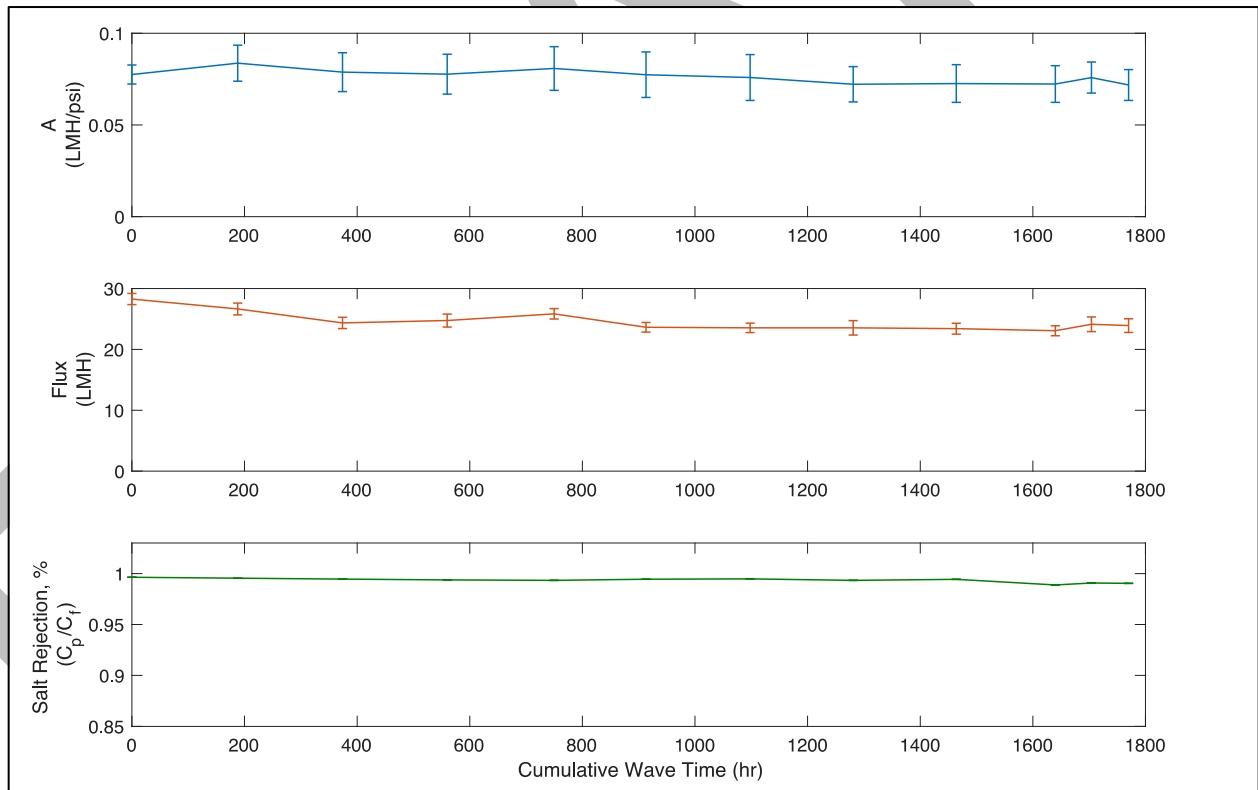


Figure 6. Water permeability coefficient (A, top frame), flux (middle frame), and salt rejection (bottom frame) for integrity tests conducted between each wave experiment.

A decline in flux over time has been previously associated with membrane fouling [34-36] in experiments with constant feed pressure. While the results in Figure 6 are from experiments at constant pressure, the wave experiments conducted under similar feed and wave conditions show no significant decline in average flux (see Table 1). Instead, this flux decline could be attributable to continuing membrane compaction after the initial compaction procedure, as feed compositions and feed pressures increased with each experiment. Indeed, we see a large dip in flux for the first three integrity tests, after which it is more consistent between each consecutive integrity test. These results present further evidence that the membrane integrity and performance was not impacted to a large degree by the variable feed pressure experiments described previously in section 3.1.1 and 3.1.3.

Deteriorating membrane flux is typically associated with some form of membrane fouling, be it biological, inorganic, or particulate/colloidal in nature [36]. It is also unclear the degree to which concentration polarization impacts these results. Concentration polarization occurs under steady operating conditions when the concentration of solutes is higher in the immediate vicinity of the membrane surface in the feed channel. This causes precipitation of solutes on the membrane surface, inducing fouling, reducing membrane flux, and lower quality permeate [36]. This phenomenon is typically observed under steady operating conditions but has never been studied under the variable flow conditions described in these experiments. It is possible that the constant variations in cross-flow velocity due to variable feed pressure cause sufficient mixing in the feed channel to mitigate some of the deleterious effects of concentration polarization. Ramakul et al. [37] found reduced concentration polarization in experiments with pulsed flow periodic operation of hollow fiber-supported liquid membrane for separation of lanthanide metal. The proposed mechanism was disturbing the boundary layer between the feed solution and membrane by

variations in flow. Similar results and rationale were published by Kennedy et al. [22] who observed increase permeation rates with pulsed flow over non-pulsed flow, and that this effect was stronger with higher frequency of pulses. Comparable results have been obtained and modelled by others, as well [17, 18, 20, 21, 23]. Therefore, it is possible that varying pressure in this manner reduces the fouling effects of concentration polarization. Though it is not a primary objective of wave-driven RO, it is a valuable side effect that warrants additional examination in later experiments.

3.3 Cation and anion rejection in permeate

The rejection efficiencies for the cations are shown in Figure 7 for the three wave periods studied with Instant Ocean and the rejection efficiencies for Cl and Br are shown in Figure 8 for the same sets of experiments. Cation and anion rejection results for the experiment using the NREL wave form (section 3.1.3) is presented in the SI as Figure SI-2 and Figure SI-3 and are not markedly different than those presented in Figure 7 and 8, highlighting the ability of a WPDS to achieve high rejections under varied conditions. Of the nine experiments conducted for 7 days, four were conducted with Instant Ocean. Boron was rejected at a lower rate than other cations. Average rejection during the constant flux periods was $85.8 \pm 2.5\%$ and $88.4 \pm 0.6\%$ for the wave periods. The higher average rejection during wave phase can be explained by the higher pressures experienced during these periods, as boron rejection is higher at higher pressures [38, 39]. No significant decreases in boron rejection were observed between the starting and ending constant flux periods. The largest observed difference was a 2.6% increase during the constant flux periods for the 7.5 wave/min experiment, reflecting a permeate boron concentration decrease of 0.1 mg/L. Boron rejection was also not markedly different as a result of wave frequency. The average of the

three wave samples for the 7.5, 1.25, and 12 wave/min experiments was $88.5\pm0.7\%$, $88.1\pm0.8\%$, and $88.7\pm0.3\%$, respectively.

DRAFT

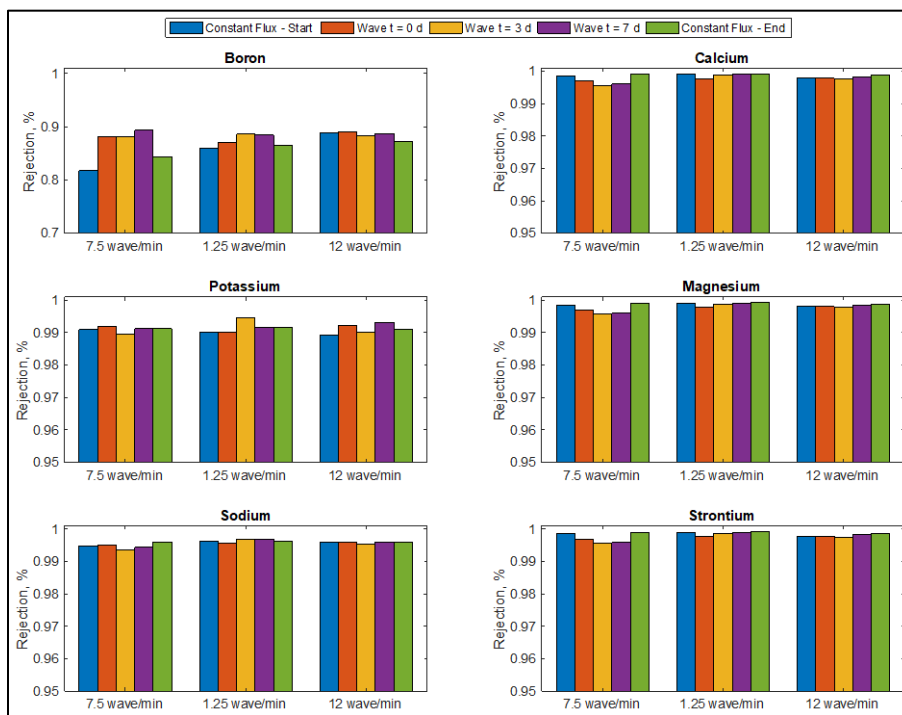


Figure 7. Rejection efficiencies for B, Ca, K, Mg, Na, and Sr for experiments conducted with Instant Ocean.

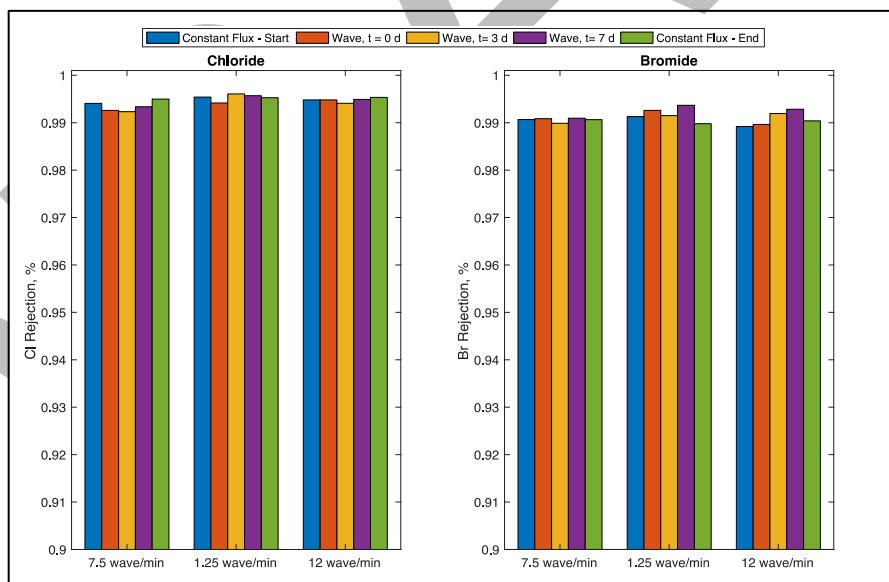


Figure 8. Rejection efficiencies for Cl and Br for experiments conducted with Instant Ocean.

For the other cations, rejections of divalent cations (Ca, Mg, Sr) were slightly higher than those for monovalent cations (K, Na), as is expected. Rejection was 99.0-99.6% for K and Na during both constant flux and wave phase. For divalent cations, rejection was 99.6-99.8% throughout the entirety of each experiment. These results show that the variable feed pressure due to the simulated waves was not a detriment to membrane performance and that the membrane performed as might be expected under constant feed pressure conditions. Cl and Br rejection were high and as would be expected under a constant pressure operating condition. Average rejection for Cl was 99.5% and for Br was 99.1%. Table SI-2 and SI-3 in the supplemental information contains the average concentration for each of these elements for both the constant flux phase and wave phase of these experiments, as well as the WHO guideline concentrations for drinking and irrigation water, where available. The permeate concentrations for each element for all experiments with Instant Ocean met these guidelines, but the experiment with concentrated Instant Ocean exceeded the drinking water guidelines for boron and sodium.

The cation rejection for the experiment conducted with 1.5× Instant Ocean are shown in Figure 9 and anion rejections are shown in Figure 10. Cation and anion rejection were consistent throughout the experiment. The trend is similar to those experiments conducted with normal concentration: boron had the lowest rejection ($81.5 \pm 1.1\%$) followed by the monovalent cations (K and Na, $>98.7\%$) and then the divalent cations (Ca, Mg, and Sr, $>99.2\%$). Br rejection averaged 98.5% and Cl rejection averaged 98.9%. Lower rejections overall can be attributed to the higher salinity feed used for this experiment. The lower rejection observed for all elements for the $t = 0$ d wave sample (Figure 9, red bar) can be attributed to the surge in permeate conductivity observed after the system was switched from constant flux mode to wave mode (e.g. see bottom right panel, Figure 4). This sample was collected for each experiment within minutes of making the switch

from constant flux to wave mode, so it is likely collected during that period the permeate conductivity had surged. There was no ending constant flux period due to experimental system failure (not membrane failure), so we cannot make any comparison, though there is no clear decline in rejection for either cations or anions over the course of the experiment.

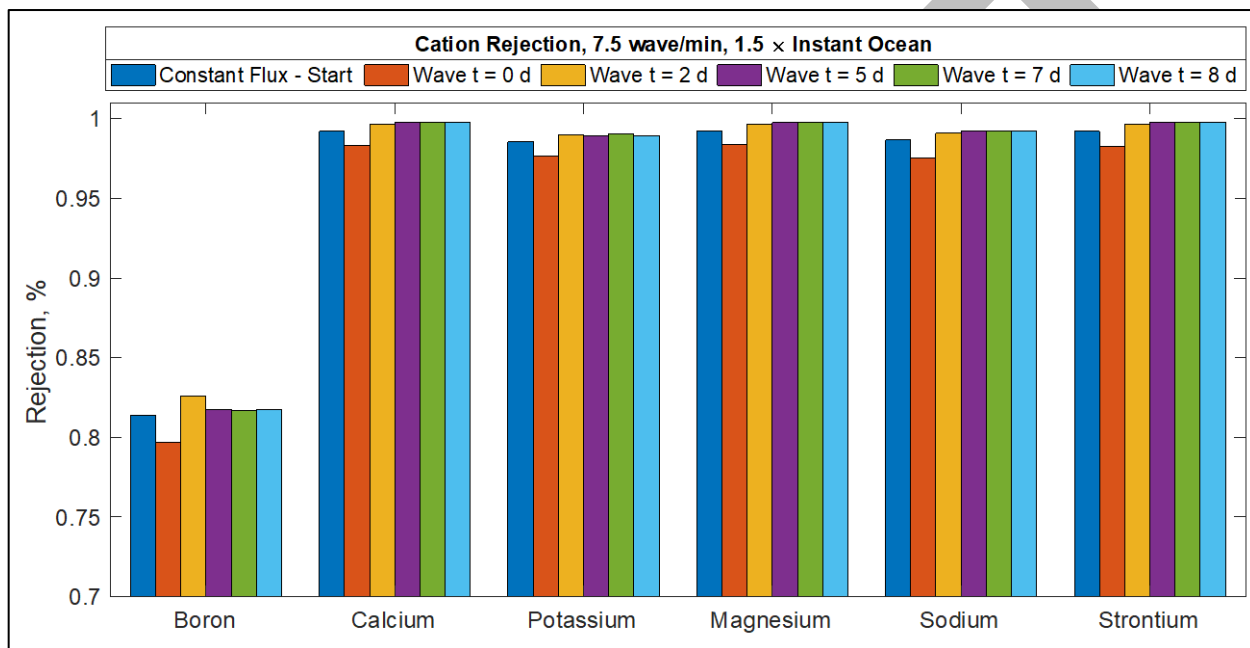


Figure 9: Rejection efficiencies for B, Ca, K, Mg, Na, and Sr for experiments conducted with 1.5x Instant Ocean.

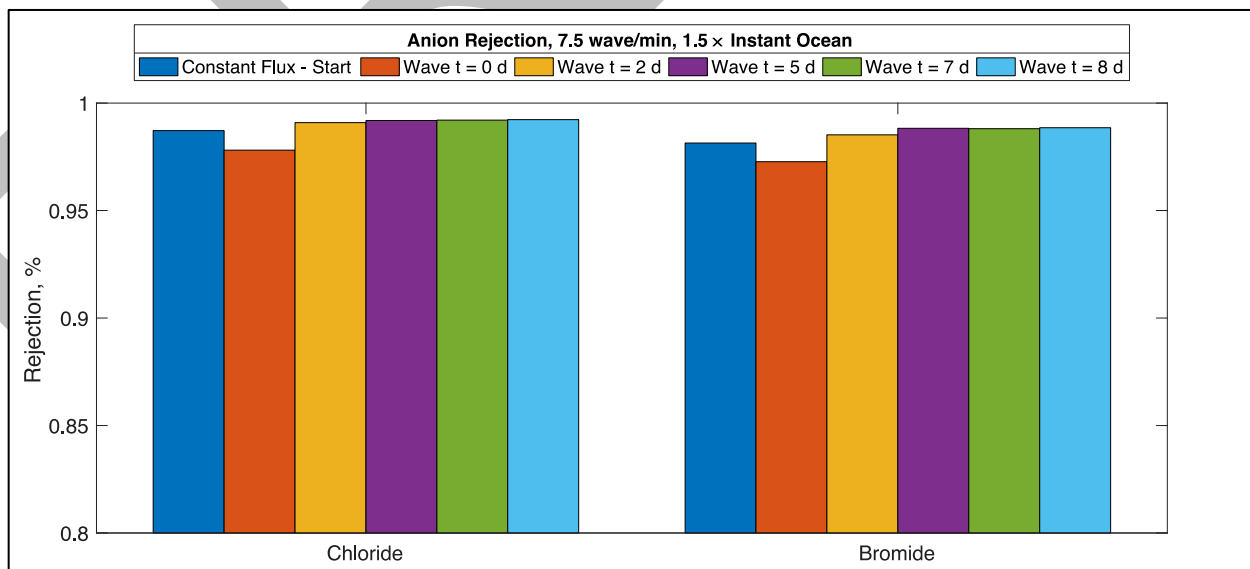


Figure 10: Rejection efficiencies for Cl and Br for experiments conducted with 1.5× Instant Ocean.

For each of these experiments, the feed pressure was variable, resulting in variable flux over the spectrum of feed pressures. The concentrations of major cations are shown in Figure 11 and the concentrations of Cl and Br are shown in Figure 12 over the spectrum of fluxes in each of the experiments. The gray line on each plot represents the average concentration for each element for all experiments with Instant Ocean. These results show that at lower fluxes, the concentration of some of these elements may produce water that is either unsafe or unpalatable. For example, the average boron concentration in three experiments was 0.58 mg/L, which is slightly above the WHO guideline of 0.50 mg/L, for flux between approximately 14-35 LMH. These samples were composite samples so were intended to reflect what the concentration might be for the end user after going into water storage and/or to the distribution system. However, these were very controlled experiments that virtually guaranteed those conditions; in a deployed system, the permeate quality will be entirely dependent on the sea state. Thus, if the system is producing water with acceptable boron content at typical conditions of 14-35 LMH, the quality of water may decline for a less energetic sea condition that produced flux of, for example, 10-25 LMH. The same could be said for other ions and the impact on palatability. In a taste test, panelists found water with >800 mg/L TDS to be the least palatable, and it was particularly influenced by high concentrations of Na, K, and Cl [40]. Perhaps the biggest risk in operating a system that runs on variable feed pressure is not the impact to the membrane but planning for variable sea conditions. If the system is in a location where low flux and feed pressure is a possibility, the system should be designed with that in mind and possibly a method for ensuring a minimum flux condition.

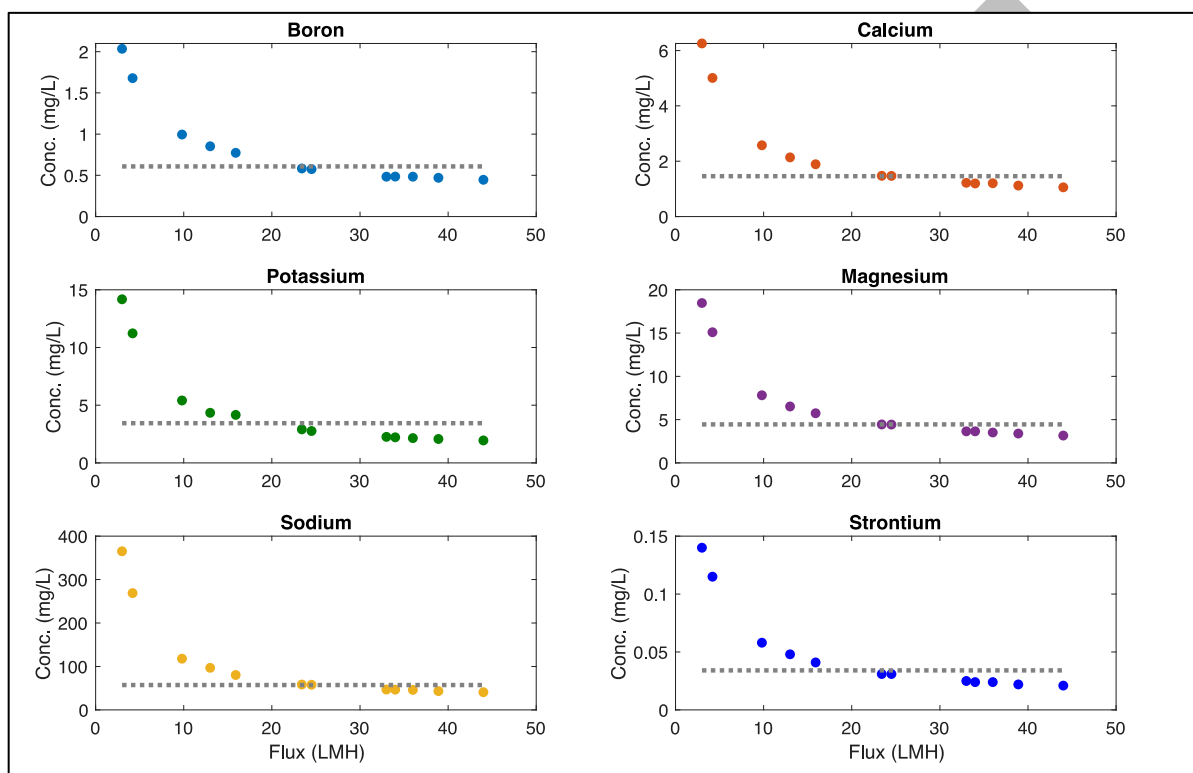


Figure 11: The concentration of B, Ca, K, Mg, Na, and Sr in permeate water spanning the fluxes seen in each experiment. Gray line represents the average permeate concentration in all experiments with Instant Ocean.

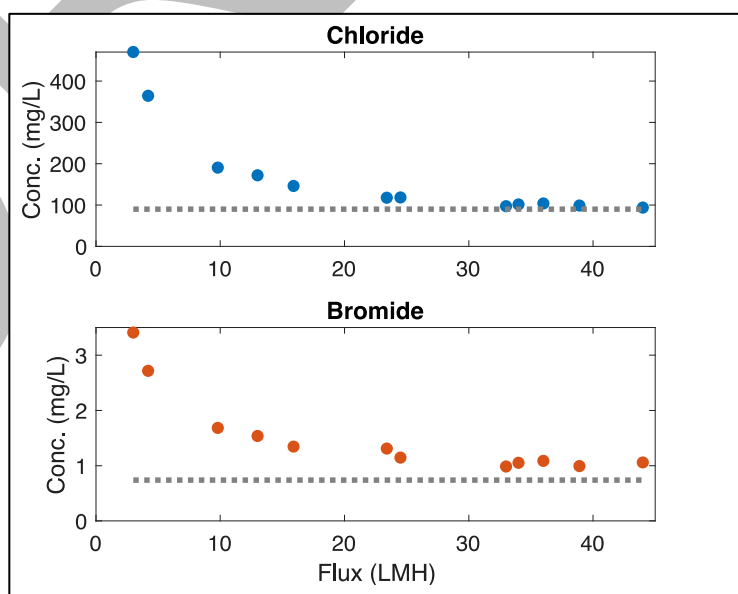


Figure 12: The concentration of Cl and Br in permeate water spanning the fluxes seen in each experiment. Gray line represents the average permeate concentration in all experiments with Instant Ocean.

4. Conclusion

This research presents results of RO experiments conducted with feed pressure swings up to 400 psi (27.5 bar) using feed compositions of NaCl and synthetic seawater. These experiments provide a baseline understanding of the impacts of consistent large pressure swings on membrane integrity and permeate quality that are needed to further development of WPDS. Membrane integrity was not shown to be impacted significantly from variable feed pressure experiments evidenced by minimal changes in critical performance parameters, such as the water permeability coefficient, calculated during constant flux periods and between each experiment. In addition, though permeate conductivity varied as expected with increasing and decreasing feed pressure, cation and anion rejections and concentrations in product water fell in expected and acceptable ranges. Wave conditions also impacted permeate quality with slower waves yielding lower salinity permeate, suggesting that a WPDS could benefit from inclusion of technology capable of smoothing the power output from higher wave periods if they are present. These results present no indication that further development in membrane technology is needed to continue research in this area. In many ways, the results presented here are unremarkable. This is a welcome result of experiments for which more membrane deterioration could be hypothesized, but the membrane behaved as might be expected if the experiments were run under typical constant feed conditions. Experimentation built on this work should include multi-element configurations, longer term trials with different membrane modules, and further experimentation with more realistic wave forms than simple sine waves.

A wave powered desalination system has many potential applications and can be part of the broader technological leap needed to bring safe drinking water to more people while reducing greenhouse gas emissions. It also has other potential applications including for quick deployment to coastal areas impacted by natural disasters and military installations. Because energy consumption accounts for the bulk of desalination cost, systems coupled with a large sustainable energy resource could reduce the specific energy consumption and, therefore, the unit cost of water delivered. Further, using wave energy directly to pressure feed water eliminates the need for some components typically found in current systems such as a turbine, electrical generator, electric motor, and hydraulic pump, likely resulting in more efficient energy use. There are also potential cost savings associated with brine disposal for a WPDS because the system would be located in, or in very close proximity to, its brine disposal point (the ocean). Thus, the possible energy and cost savings from a fully realized WPDS warrant continued research and development in this area and results from this work invite many more research questions.

Research towards development of wave-powered RO systems are still in the beginning stages. This research represents the first step of many toward not only fabricating and deploying a WPDS, but also understanding the membrane processes and phenomena in play. However, more fundamental and baseline research should be conducted before engaging in system design. Much of what is understood about membrane processes assumes a constant feed condition; but when that changes, established concepts need to be reevaluated. Research is needed on the fouling and scaling tendencies of a membrane subject to wide pressure variations because fouling and scaling are significant considerations for engineering membrane treatment systems and can impact feed pressure itself. Similarly, concentration polarization results from constant feed pressure and flow but should be better understood when operating under variable feed conditions. Further

understanding and experimentation of larger design concepts, like membrane element configuration and process flow, will help build on the results presented here. Efforts to understand these phenomena under potential WPDS conditions will aid in system design, membrane technology development, and modelling efforts. Aside from technology fundamentals, deploying a WPDS presents a new paradigm for membrane technology scientists and engineers. Like any other RO system, feed water in a WPDS needs to undergo some type of pretreatment. This presents unique challenges for a system that could exist entirely underwater and a pretreatment technology that would be subject to variable feed conditions itself. There are similar challenges presented for system maintenance, product water distribution and delivery, and other aspects of water treatment engineering past the treatment.

Acknowledgements:

The authors would like to thank and acknowledge our collaboration with the National Renewable Energy Laboratory for funding support during the preparation of this manuscript. This work was also supported by _____. Additionally, the authors would like to thank Michael Veres and Tani Cath for their design and fabrication of the system used to conduct these experiments and continued assistance with troubleshooting and system maintenance.

References

1. Li, Z., et al., *Towards sustainability in water-energy nexus: Ocean energy for seawater desalination*. Renewable and Sustainable Energy Reviews, 2018. **82**: p. 3833-3847.
2. Abdelkareem, M.A., et al., *Recent progress in the use of renewable energy sources to power water desalination plants*. Desalination, 2018. **435**: p. 97-113.
3. Ma, Q. and H. Lu, *Wind energy technologies integrated with desalination systems: Review and state-of-the-art*. Desalination, 2011. **277**(1-3): p. 274-280.
4. Miranda, M.S. and D. Infield, *A wind-powered seawater reverse-osmosis system without batteries*. Desalination, 2003. **153**(1-3): p. 9-16.
5. Subiela, V.J., J.A. Carta, and J. González, *The SDAWES project: lessons learnt from an innovative project*. Desalination, 2004. **168**: p. 39-47.
6. Freire-Gormaly, M. and A.M. Bilton, *Experimental quantification of the effect of intermittent operation on membrane performance of solar powered reverse osmosis desalination systems*. Desalination, 2018. **435**: p. 188-197.
7. Valladares Linares, R., et al., *Forward osmosis niches in seawater desalination and wastewater reuse*. Water Res, 2014. **66**: p. 122-139.
8. Folley, M., B. Peñate Suarez, and T. Whittaker, *An autonomous wave-powered desalination system*. Desalination, 2008. **220**(1-3): p. 412-421.
9. Leijon, J. and C. Boström, *Freshwater production from the motion of ocean waves – A review*. Desalination, 2018. **435**: p. 161-171.
10. Sharmila, N., et al., *Wave powered desalination system*. Energy, 2004. **29**(11): p. 1659-1672.
11. Leijon, J., et al., *Marine Current Energy Converters to Power a Reverse Osmosis Desalination Plant*. Energies, 2018. **11**(11): p. 2880.
12. Qasim, M., et al., *Reverse osmosis desalination: A state-of-the-art review*. Desalination, 2019. **459**: p. 59-104.
13. Wang, K., et al., *Mechanical properties of water desalination and wastewater treatment membranes*. Desalination, 2017. **401**: p. 190-205.
14. Jiang, S., Y. Li, and B.P. Ladewig, *A review of reverse osmosis membrane fouling and control strategies*. Sci Total Environ, 2017. **595**: p. 567-583.
15. Yu, Y.-H. and D.S. Jenne, *Analysis of a Wave-Powered, Reverse-Osmosis System and Its Economic Availability in the United States*, in *American Society of Mechanical Engineers' International Conference on Ocean, Offshore and Arctic Engineering*. 2017: Trondheim, Norway.
16. Cornett, A.M., *A Global Wave Energy Resource Assessment*, in *The Eighteenth International Offshore and Polar Engineering Conference*. 2008, International Society of Offshore and Polar Engineers: Vancouver, Canada.
17. Al-haj Ali, M., et al., *Optimization-based periodic forcing of RO desalination process for improved performance*. Desalination and Water Treatment, 2013. **51**(37-39): p. 6961-6969.
18. Emad, A., A. Ajbar, and I. Almutaz, *Periodic control of a reverse osmosis desalination process*. Journal of Process Control, 2012. **22**(1): p. 218-227.
19. Abufayed, A.A., *Performance characteristics of a cyclically operated seawater desalination plant in Tajoura, Libya*. Desalination, 2003. **156**(1-3): p. 59-65.
20. Al-Bastaki, N.M. and A. Abbas, *Periodic Operation of a Reverse Osmosis Water Desalination Unit*. Separation Science and Technology, 1998. **33**(16): p. 2531-2540.

21. Al-Bastaki, N.M. and A. Abbas, *Improving the permeate flux by unsteady operation of a RO desalination unit*. Desalination, 1999. **123**(2-3): p. 173-176.
22. Kennedy, T.J., R.L. Merson, and B.J. McCoy, *Improving permeation flux by pulsed reverse osmosis*. Chemical Engineering Science, 1974. **29**(9): p. 1927-1931.
23. Abbas, A. and N. Al-Bastaki, *Flux enhancement of RO desalination processes*. Desalination, 2000. **132**(1-3): p. 21-27.
24. Ali, M.A.-h., et al., *Study of cyclic operation of RO desalination process*. The Canadian Journal of Chemical Engineering, 2011. **89**(2): p. 299-303.
25. Yu, Y.-H. and D. Jenne, *Numerical Modeling and Dynamic Analysis of a Wave-Powered Reverse-Osmosis System*. Journal of Marine Science and Engineering, 2018. **6**(4): p. 132.
26. Cath, T.Y., et al., *Standard Methodology for Evaluating Membrane Performance in Osmotically Driven Membrane Processes*. Desalination, 2013. **312**: p. 31-38.
27. Toffoli, A. and E.M. Bitner-Gregersen, *Types of Ocean Surface Waves, Wave Classification*. 2017: p. 1-8.
28. Greenlee, L.F., et al., *Reverse osmosis desalination: water sources, technology, and today's challenges*. Water Res, 2009. **43**(9): p. 2317-48.
29. Kim, J., et al., *A comprehensive review of energy consumption of seawater reverse osmosis desalination plants*. Applied Energy, 2019. **254**: p. 113652.
30. Davies, P.A., *Wave-powered desalination: resource assessment and review of technology*. Desalination, 2005. **186**(1-3): p. 97-109.
31. Kim, S., *Osmotic pressure-driven backwash in a pilot-scale reverse osmosis plant*. Desalination and Water Treatment, 2013. **52**(4-6): p. 580-588.
32. Sagiv, A. and R. Semiat, *Backwash of RO spiral wound membranes*. Desalination, 2005. **179**(1-3): p. 1-9.
33. Panagopoulos, A., K.J. Haralambous, and M. Loizidou, *Desalination brine disposal methods and treatment technologies - A review*. Sci Total Environ, 2019. **693**: p. 133545.
34. Mohammadi, T., M. Kazemimoghadam, and M. Saadabadi, *Modeling of membrane fouling and flux decline in reverse osmosis during separation of oil in water emulsions*. Desalination, 2003. **157**(1-3): p. 369-375.
35. Maltos, R.A., et al., *Produced water impact on membrane integrity during extended pilot testing of forward osmosis – reverse osmosis treatment*. Desalination, 2018. **440**: p. 99-110.
36. Guo, W., H.H. Ngo, and J. Li, *A mini-review on membrane fouling*. Bioresour Technol, 2012. **122**: p. 27-34.
37. Ramakul, P., et al., *Reduction of concentration polarization at feeding interphase of a hollow fiber supported liquid membrane by using periodic operation*. Korean Journal of Chemical Engineering, 2009. **26**(3): p. 765-769.
38. Patroklou, G., K.M. Sassi, and I.M. Mujtaba, *Simulation of boron rejection by seawater reverse osmosis desalination*, in *The 11th International Conference on Chemical and Process Engineering*. 2013, AIDIC: Milan, Italy. p. 281-290.
39. Prats, D., M.F. Chillon-Arias, and M. Rodriguez-Pastor, *Analysis of the influence of pH and pressure on the elimination of boron in reverse osmosis*. Desalination, 2000. **128**(3): p. 269-273.
40. Platikanov, S., et al., *Influence of minerals on the taste of bottled and tap water: a chemometric approach*. Water Res, 2013. **47**(2): p. 693-704.